# Real-Time Highly Resolved Spatial-Temporal Vehicle Energy Consumption Estimation Using Machine Learning and Probe Data

Joseph Severino[1], Yi Hou[1], Ambarish Nag[1], Jacob Holden[1], Lei Zhu[2], Juliette Ugirurmurera[1], Stanley Young[1], Wesley Jones[1], and Jibonananda Sanyal[3]

[1]National Renewable Energy Laboratory, Golden, CO
[2]University of North Carolina-Charlotte, Charlotte, NC
[3]Oak Ridge National Laboratory, Oak Ridge, TN

**Abstract**

Real-time highly resolved spatial-temporal vehicle energy consumption is a key missing dimension in transportation data. Most roadway link-level vehicle energy consumption data are estimated using average annual daily traffic measures derived from the Highway Performance Monitoring System; however, this method does not reflect day-to-day energy consumption fluctuations. As transportation planners and operators are becoming more environmentally attentive, they need accurate real-time link-level vehicle energy consumption data to assess energy and emissions; to incentivize energy-efficient routing; and to estimate energy impact caused by congestion, major events, and severe weather. This paper presents a computational workflow to automate the estimation of time-resolved vehicle energy consumption for each link in a road network of interest using vehicle probe speed and count data in conjunction with machine learning methods in real time. The real-time pipeline can deliver energy estimates within a couple seconds on query to its interface. The proposed method was evaluated on the transportation network of the metropolitan area of Chattanooga, Tennessee. The volume estimation results were validated with ground truth traffic volume data collected in the field. To demonstrate the effectiveness of the proposed method, the energy consumption pipeline was applied to real-world data to quantify road transportation-related energy reduction because of mitigation policies to slow the spread of COVID-19 and to measure energy loss resulting from congestion.

**Acknowledgement**

This work was authored by the National Renewable Energy Laboratory, operated by Alliance for Sustainable Energy, LLC, for the U.S. Department of Energy (DOE) under Contract No. DE-AC36-08GO28308.

Transportation accounts for up to 28% of total energy usage and 33% of total carbon gas emissions in the United States (*1*, *2*). In 2017, more than 3.3 billion gallons of fuel and approximately 8.8 billion hours of productivity are lost because of highway congestion in the United States alone (*3*). The United Nations (*4*) estimated that approximately 70% of the world population will be living in urban areas by 2050. The surge in the population in fast-growing urban areas will lead to more congestion, more energy waste, and more carbon gas emissions. Consequently, transportation agencies have set sustainability goals to building energy-efficient and low-carbon mobility systems. To achieve such goals, it is critical to have the capability to estimate energy consumption. The energy consumed can then be converted into carbon emissions of all vehicles in transportation networks in cities. Such capabilities can be used not only to establish baselines but also to evaluate the effectiveness of related policies. Having high-resolution vehicle energy estimates along with speed and volume data on every road link enables the evaluation of the energy cost associated with delays in mobility. Moreover, real-time link-level energy estimates are the foundation of providing alternative routing opportunities for personal and commercial mobility modes. This can be accomplished by enabling energy-aware routing algorithms. These algorithms for routing would complement existing routes based on the shortest paths and shortest travel times. During the ongoing COVID-19 pandemic, cities and transportation agencies are interested in quantifying the impacts of COVID-19 on transportation. Having access to high-resolution vehicle energy estimates can help agencies quantify impacts through the lens of vehicle energy consumption.

An integral part of any vehicle energy estimation model for the prediction of energy consumption under real-world circumstances is the speed profile or driving cycle of vehicles (*5*–*7*). Speed profiles for real-world vehicle energy prediction are often presented in a discrete set of drive cycles or a combination of these drive cycles (*8*, *9*). Although high-frequency (approximately 1-Hz) drive cycles are critical for high-resolution vehicle power train simulations to determine energy consumption, it is impractical to collect these drive cycles from all vehicles on the road because external hardware and sensing equipment must be installed in each vehicle; thus, this paper proposes an automated pipeline to estimate high- resolution link-level energy consumption in the network using abstracted energy and volume estimation techniques enabled by machine learning, TomTom vehicle probe data, and a repository of real-world vehicle drive cycles. TomTom is a data provider of traffic data, including anonymous probe count and hourly historic speed aggregates mapped to network links (*10*).

The main contributions of this paper are (1) to present highly resolved temporal and spatial vehicle energy estimation at road link level, (2) to develop a machine learning-based workflow with high accuracy for traffic volume and energy estimation, (3) to provide a tool for estimating real-time vehicle energy estimation that can enable real-time energy-aware routing decision (*11*, *12*) and traffic management (*13*, *14*), and (4) to provide policymakers with tools to evaluate policies to reduce road transportation-related energy demand. The remainder of the paper is organized as follows. A summary of the extensive literature review is described in the next section. A detailed description of the proposed energy estimation pipeline is then presented, followed by a section presenting the model results. The results section reports the accuracy and validation process for both traffic volumes and energy estimation, and it demonstrates road transportation-related energy reduction resulting from mitigation policies to slow the spread of COVID-19 and an analysis of energy loss attributable to traffic congestion. Finally, the paper concludes with a discussion of the advantages of the proposed method and directions for future research.

**Literature Review**

Vehicle energy estimation is critical to vehicle range prediction, power train optimization, and energy-efficient routing. Because of its importance, vehicle energy estimation has been a popular research topic in transportation for many years. Most work in this field has focused on energy consumption by electric vehicles, though there have been some studies related to liquid-fueled vehicles. These models are either physics based or data based—or, in some cases, a combination of both. Moreover, most of these models provide energy consumption for the whole trip, and only a few of these models provide estimates of the energy consumption at the resolution of each road link or segment that constitutes the trip.

In the field of electric vehicles, vehicle energy estimation models have been created for the design and optimization

of electric vehicle drivetrains (*15–17*), the assessment of real-world driving conditions on electric vehicle energy consumption (*18*, *19*), the impact on global energy consumption or the electric grid resulting from the introduction of electric vehicles or hybrid power train vehicles (*20–22*), and the range prediction for all-electric vehicles (*23*). There are also studies that focused on modeling the consumption behavior of liquid-fueled internal combustion engine vehicles (*24*, *25*).

Energy estimation with the goal of range prediction either uses statistical models or relies on drivetrain and vehicle behavior simulations, sometimes down to the component level (*5*, *26*, *27*). Vehicle simulation models require calibration and validation using real-life tests or roller bench tests, and they use detailed speed profiles or drive cycles as input for estimation. On the other hand, statistical models require real-world travel data and differ in the extent to which they can be connected to the underlying physical principles and speed profiles (*15, 28–30*). Zhao et al. developed a smartphone application for the real-time prediction of vehicular fuel consumption that uses a digital map application programming interface (API) to forecast traffic conditions and the trip time of each route (*31*). Their fuel consumption model is based on the vehicle-specific power distribution, which can connect the traffic condition and trip time with vehicular engine displacement to model vehicular fuel consumption.

Few studies have focused on roadway link-level vehicle energy estimation. Kraschl-Hirschmann and Fellendorf developed an approach to calculate link-level energy consumption based on the actual power needed to overcome the driving resistance for each link and using link travel speeds and volume-to-capacity ratios (*24*). This method can be embedded in routing algorithms and used as one component in the optimization of the route algorithm's generalized cost function. Recently, Holden et al. developed the Route Energy pre- diction Model (RouteE) for the accurate estimation of energy consumption for a variety of vehicle types (i.e., makes and models) over trips or sub-trips where detailed drive cycle data are unavailable (*32*). The RouteE models were established using the Future Automotive Systems Technology Simulator (FASTSim) paired with approximately 1 million miles of drive cycle data across the United States from the Transportation Secure Data Center (*33*). These models were thus trained for specific vehicle makes and models. Because the training drive cycle data are representative of various driving conditions in United States including Tennessee, these models were directly applied to link-level vehicular energy estimation for Chattanooga, TN. Although existing methods have proven to be effective in estimating link-level energy consumption for a single vehicle, they are incapable of estimating total vehicle energy consumption on each roadway link.

## Methods

The energy estimation pipeline comprises five main components, as shown in Figure 1: constructing and validating a base network's spatial attributes; matching TomTom links to the base network; estimating real-time link-based volume and speed using TomTom speed and probe count data; predicting real-time vehicle energy consumption using RouteE models; and visualizing geospatial link-wise vehicle energy consumption. The base network construction and map-matching steps are per- formed offline and need to happen only once to initialize the workflow. The speed and energy estimation processes are performed continuously in real time as new TomTom segment data become available. As mentioned, once the workflow is established, it takes only a few seconds to generate new real-time energy estimates given new real- time data. The visualization step enables the analysis of various scenarios, both historically and in near-real time, and it is performed offline by first collecting the energy estimate data of interest. Further details on the different steps of our methodology are provided below.

### *Construct and Validate Base Network Attributes*

The first step in the pipeline, as displayed in Figure 1, represents the cleaning and construction of a base net- work. In this step, we combined elevation data with each link. The base network considered in our study was provided by the City of Chattanooga, Tennessee, Transportation Planning Organization (TPO). The data included more than 36,000 links with 150 features. We were able to complement this base network with other sources of data, including the contour elevation TIF files, to provide elevations at the beginning and end of each link. The knowledge of these elevations enabled us to calculate the change in grade percentage along each road segment so that we could evaluate

energy more accurately. This network also includes functional road classifications, which are used to group roads according to the character of service they are intended to provide. These attributes are useful to improve energy estimations by accounting for spatial differences among various links.

*Match Networks*

After establishing a base network, we matched this network to the TomTom network to easily join the TomTom data to the base network in real time (refer to Figure 1). We combine these networks to preserve all the features from each network, thus enabling a comprehensive analysis. Various network-matching algorithms are used to address various scenarios (34, 35), but line-based methods that analyze line segment properties are most commonly used (36). Similarly, we developed a simplified algorithm to match two network shapefiles with mixed bidirectional geometries by combining threeline segment metrics: the minimum distance of geometries ($d_{min,ij}$), the Hausdorff distance ($d_{max,ij}$), and the difference in linestring azimuth ( $\Delta_{\varphi ij}$).

The minimum distance of geometries is the minimum distance between two linestrings, where a linestring is a one-dimensional object representing sequential points and the line connecting them. This metric is not sufficient to exclude matching connected and perpendicular links because these links would have a distance of zero; therefore, we also used the Hausdorff distance, which measures the maximum distance of a linestring to the nearest point in the other linestring, thereby providing a way to find links with the most overlap. Last, we determined the azimuth (shown in Figure 2), which is the angular measurement in a spherical system, for each link in network. We then calculate the difference in azimuth between each pair of links to account for the deviation in link directions. The algorithm works by summing the values of these three metrics for a link *i* in the TPO network compared with every link *j* in the TomTom network, as shown in Equation 1. The lowest sum over all pairs corresponded to a matching pair of links from the two networks. In the example below (Figure 2), we see two pairs of segments (links): ($A_i$,$B_j$) and ($C_j$,$D_i$). Once more, links with subscript *i* represent links contained in the base TPO network and subscript *j* represent the TomTom network segments. When we look at link $A_i$ and $B_j$, we see an example where two links are touching each other and both going in the same direction. Here, the minimum distance (i.e., $\|d_{min,\,ij}\|$) would be zero and the $\|\Delta_{\varphi,ij}\|$ would be zero as well. However, the $\|d_{max,ij}\|$ would be greater than zero, making this pair suboptimal. The ideal match would have all distance metrics equal to zero or relatively small for best pairing. Another scenario is demonstrated here looking at links $C_j$ and $D_j$ to show the links that are relatively close but traveling in different directions. This would aggregate with an error significantly greater than zero, making it less optimal of a match.

$$arg\ min_{i,\,j}\left(\left\|d_{max,\,ij}\right\| + \left\|d_{min,\,ij}\right\| + \left\|\Delta\varphi_{ij}\right\|\right) \qquad (1)$$

where *i* is a link in the TPO network, and *j* is a link in the TomTom network,

$\|d_{max,\,ij}\|$ is the magnitude of the Hausdorff distance between links *i* and *j*,

$\|d_{min,\,ij}\|$ is the magnitude of the minimum distance between links *i* and *j*, and

$\|\Delta_{\varphi ij}\|$ is the magnitude of the difference in azimuth between links *i* and *j*:

Ideally, the lowest sum value would be zero; zero minimum distance corresponds to links that at least touch each other; a Hausdorff distance of zero means that every point along the two linestrings are shared; and, last, an azimuth difference of zero signifies two links oriented in the same direction. We found this method to be highly effective, with 97% accuracy for a small sample of the base network. The small network was centered at Figure 2 and comprised 160 road segments for our base TPO network and 250 segments for the TomTom network. This accuracy makes sense as the TomTom network was broken up into smaller road segments. This meant there were typically one or more TomTom segments contained in one TPO segment. Thus, having a zero distance between them was easy to find and determining the minimum

azimuth difference was needed to find the best match. This exhaustive algorithm is computationally expensive when applied to the whole base network; thus, we partitioned the networks into equal-size grids. With this partitioning, a link in a grid g was compared only with links in grid g or to grids adjacent to g, thus reducing the computational time (see Figure 3). Partitioning the network also adds to the accuracy of the algorithm, as it only searches for links within a reasonable proximity to the given segment under analysis.

*Estimate Real-Time Traffic Volume*

Next, we estimated volume (i.e., number of vehicles) of the current hour on every link on the roadway network, a crucial step in this study. We used the methodology developed by Hou et al. (*37*, *38*) for historical traffic volume estimation. Hou et al. leveraged the advanced machine learning method—Extreme Gradient Boosting (XGBoost) (*39*)—to generate link-level traffic volume using TomTom probe counts (the number of Global Positioning System devices captured by TomTom) and speed profiles along with various other exogenous data, including weather information (temperature, wind speed, precipitation, and snow), road characteristics (speed limit and road class), and temporal information (time of day, day of week). XGBoost received enormous recognition in a few machine learning and data mining challenges in the past decade for its high prediction accuracy. The most prominent feature of XGBoost is scalability. XGBoost is competent in parallel learning. It can use multiple Computing Processing Unit threads with the efficient use of a ‘‘cache aware’’ mechanism (*39*). Compared with deep learning, XGBoost has fewer hyperparameters to tune and is more computationally efficient as it requires fewer data for training. The historic traffic volume estimation method was then modified to enable real-time traffic volume estimation. The challenge for real-time volume estimation is the availability of real-time streaming probe count and speed data. Real-time speed data can be queried from TomTom live feed API every minute, but probe count data provided by TomTom has a latency of approximately 24 h and is not in real time. An alternative is to use only historical probe counts instead of real-time

probe counts; thus, for the model inputs for the real-time traffic volume estimation, we use the probe count of the same hour of day and same day of week in the last week and the average probe count of the same hour of day and same day of week for the past month.

*Estimate RouteE Energy*

Provided real-time speeds, volumes, grade, and link length, we have sufficient information to calculate near-real-time energy consumed on each segment of road using the National Renewable Energy Laboratory’s RouteE software (*32*). RouteE considers link features— such as average traffic speed, road grade, and link length—to accurately estimate energy consumption for particular vehicle types. RouteE models are trained on energy consumption data from roughly 1 million miles of real-world driving data housed in the Transportation Secure Data Center (*29*). Consideration of traffic speed and the flexibility to include other time-variant features allows RouteE to predict energy consumption that accounts for changing real-time conditions. Inputs to RouteE include the average speed of vehicles traversing the link, the average grade across a link, and the length of the link. In our study, we used RouteE for conven- tional, hybrid electric, plug-in hybrid electric, and battery electric vehicles.

The RouteE methodology is applicable to light-, medium-, and heavy-duty vehicles. In this work, energy predictions for both passenger cars and a Class 8 line- haul truck are generated. RouteE offers different estimator types—including explicit bin (lookup tables), linear regressors, and random forest regressors—that are best suited to different applications. In this pipeline, we used the random forest regressors because this was the most robust model for interpolating among discrete conditions (feature sets) captured in the original training data as documented in RouteE literature (*32*). The model features used in each estimator type are the average speed over a link in miles per hour (mph), the average grade across a link as a percentage, and the length of the link in miles

## Results

As mentioned, we evaluated the pipeline for the Chattanooga, Tennessee, metropolitan area. First, a link-level traffic volume estimation model was developed and validated using vehicle probe count data. Then, the RouteE energy estimation model was analyzed. Last, by combining these two models, we quantified the impacts of COVID-19 on road transportation-related energy reduction, and measured energy loss attributable to congestion to demonstrate the effectiveness of the proposed method.

### *Real-Time Volume Estimation*

The ground truth traffic volume data were collected for the Chattanooga, Tennessee, network for model training and validation from two different data sources: radar sensor data on interstates and Tennessee Department of Transportation (DOT) short-term volume count on non-interstate roads, including other freeways, principal arterials, minor arterials, major collectors, minor collectors, and local roads. The traffic volume data were observed on an hourly basis. The radar sensor data on interstate roads contain 81,918 observations and were collected at 36 locations from January 1st to April 22nd, 2019. The short-term volume count data contain 15,570 observations and were collected at 501 locations from January 3rd to June 5th, 2019. Figure 4 shows both the radar sensor locations and the locations of where the Tennessee DOT collected the short-term volume counts as well as the average traffic volume at each location. Detailed information about traffic volume estimation data sources is shown in Table 1.

Because of different data sources, separate models were developed for the interstate and non-interstate locations. Ten-fold cross-validation was adopted to validate the model training results to prevent model from overfitting and being biased, as overfitting and biased estimation affects accurately assessing the energy consumption and making decisions for policymakers. R-squared and mean absolute error (MAE) were used to evaluate the model. R-squared is known as the coefficient of determination and measures how well the data are fitted to a regression line. Values closer to zero represent a poor fit, whereas values closer to 1 represent a better fit. A lower MAE value indicates higher model accuracy and is desired. The difference between historical and real-time volume estimation is the vehicle probe counts. Historical volume estimation model takes the vehicle probe count of a given hour to estimated traffic volume of the same given hour. Because of the lack of available real-time probe counts in the market, the real-time volume estimation model takes the probe count of the same hour of day and same day of week in the last week and the average probe count of the same hour of day and same day of week for the past month to estimated traffic volume of the current hour in real time. The results for both historical and real-time volume estimation are presented in Table 2. The results indicate that the models yield R- squared values of 0.77 and 0.76 and MAEs of 76 and 79 vehicles per hour for historical and real-time volume estimation on non-interstate roadways, and R-squared values of 0.84 and 0.83 and MAEs of 236 and 242 vehicles per hour for historical and real-time volume estimation on interstate roadways. The real-time traffic volume estimation without real-time probe count has a similar model accuracy to the historical volume estimation.

### *RouteE Model Analysis*

To provide further insight into energy consumption behavior, we characterized the dependence of fuel economy on each feature used by RouteE individually. We fixed values for all features but one, and we estimated the energy consumption for a range of values of the varied feature using both the explicit bin (lookup tables) and the random forest regressor approaches. The details from this investigation are summarized in Figure 5, where the analysis of the Toyota Camry model and Class 8 line- haul diesel truck model are displayed. Simultaneous variation of the random forest model-predicted miles per gallon with both speed and grade percentage shows that the highest fuel economy values correspond to highway cruise speeds (55–65 mph) and negative grade values, as expected for a conventional power train.

### *COVID-19 Energy Impact Analysis*

We collected real-time speeds every minute on average for more than 18,000 links on the network. We used

these speeds along with other network features to generate real-time average energy estimates per vehicle on each link by applying RouteE model. Additionally, we calculated the total energy consumption on each link by multiplying the hourly average energy estimates with estimated hourly traffic volume. When estimating the total energy on each link, we used two validated vehicle models: Class 8 line-haul truck and Toyota Camry for passenger vehicles. The distribution was divided up with 9% comprising trucks and 91% passenger vehicles. This distribution was derived from video footage collected by cameras along the highways. The video data were only available for highways and there were no other data to support distributions for other road classes. Therefore, we assume this distribution for all links but understand that vehicle composition varies for each road class. The total energy per link was only analyzed using historic hourly estimates derived from average hourly speeds provided by TomTom. As the road network is arbitrarily segmented, the total energy consumption on each link is normalized by link length to produce energy intensity defined as gasoline gallon equivalent (gge) per mile.

The energy impact of the ongoing COVID-19 pandemic was analyzed. Two Wednesdays, February 19th and March 25th, 2020, were randomly selected before and during the stay-at-home orders for comparison. Figure 6 shows the real-time relative speeds around 6 p.m. for the region before (Wednesday, February 19th, 2020) and during (Wednesday, March 25th, 2020) the stay-at-home orders. Relative speed is defined as observed speed divided by free-flow speed, where free-flow speed is obtained through TomTom on each link (*40*). It is observed that the stay-at-home orders decreased the congestion on the roads during the afternoon peak near 6 p.m.

The alleviation of congestion was translated to an energy intensity decrease on the links by applying RouteE Toyota Corolla models and taking into account traffic volume. The comparison between the energy intensity before and during stay-at-home orders in the Chattanooga region is presented in Figure 7. As expected, the results show that the energy intensity for Wednesday, February 19, 2020, before the stay-at-home orders, were much higher than the energy intensity observed on March 25, 2020, when the stay-at-home orders were in effect. The total vehicle energy consumption of the network in a period of 24 h on February 19th (before stay-at-home orders) and March 25th (during stay-at-home orders), 2020 were calculated and the results are shown in Table 3. We only aggregated the vehicle energy consumption for highways and arterials, as the volume estimation model had the best performance on these road classes. The results show a total energy reduction of 30.4% and decrease in the volume of over 29.7% during stay-at-home orders. We can also see more reduction occurring on arterial than highways.

A sensitivity analysis of various vehicle models was conducted to understand the impact different fuel efficiency vehicles would have in the region. The sensitivity analysis results are shown in Figure 8. As expected, the largest gas-only vehicle, Ford Explorer, incurred the highest fuel consumption, which was nearly twice the fuel consumed of the compact hybrid electric vehicle, Ford C- Max HEV. We also observed that the Toyota Highlander hybrid, which is of similar size as the Ford Explorer, saved about 31.4% total fuel compared with the Ford Explorer.

*Congestion Energy Impact Analysis*

An energy metric, energy loss ratio, is defined as the ratio of energy consumption per vehicle per mile for the actual measured speed to the corresponding energy consumption for the free-flow speed. For each link, the free-flow speed for a given day was obtained through TomTom. Figure 9 shows link-wise energy loss ratio of the Chattanooga roadway network at 5 p.m. on February 19, 2020, using the trained Toyota Camry and Class 8 line-haul truck models. As shown in Figure 9, the Class 8 line-haul truck seems have a larger energy loss ratio than the Toyota Camry on most of the links. This could be in part because of the notion that Class 8 trucks have a significant aero drag coefficient, which makes fuel economy more sensitive to speed than in light-duty vehicles.

Next, we explored how the energy loss ratio varies with traffic congestion level, where congestion level is defined as:

$$congestion\ level = 1 - \frac{actual\ speed}{free\ flow\ speed} \qquad (2)$$

The relationship between congestion level and energy loss ratio for Toyota Camry model is shown in Figure 10. There is a rapid increase of the energy loss ratio when the congestion level approaches 0.8. This variation could be reasonably fitted, as shown in Figure 10, using an exponential function of the form $y = ae^{bx} + c$.

The energy loss (gge per mile) is defined as the difference between the energy intensity of the actual measured speed and the energy intensity of the free-flow speed, and was converted from energy loss ratio by accounting for traffic volume on each link. Figure 11 shows the energy loss caused by congestion on the links in the Chattanooga road network at 5 p.m. on February 19, 2020. As expected, most of the energy loss occurred at downtown and major corridors.

The energy loss resulting from congestion by road class was further calculated for the entire day on February 19, 2020. Consequently, we can discern which road class contains the most room for energy improvement given enhanced traffic planning and management. The results are shown in Figure 12. As shown in the figure, minor arterials, and major collectors demonstrate, on average, the most opportunity for improvement, whereas freeways and interstates reveal the least opportunity. This context would provide valuable information to local and state transportation planning entities to justify various infrastructure or control changes to improve mobility and energy consumption within their jurisdiction.

**Conclusions**

This paper presented a novel methodology for generating real-time, accurate, highly resolved spatial-temporal link-level vehicle energy estimation. The methodology is based on a pipeline with two main components: a machine learning model, XGBoost, to estimate real-time link-level traffic volume using traffic probe data; and the RouteE energy estimation model to generate real-time vehicle energy consumption. By combining the traffic volume estimated by XGBoost with the RouteE vehicle energy consumption estimate, we can estimate in near-real-time total vehicle energy consumption on each segment of a roadway network. We applied this pipeline on the Chattanooga, Tennessee, regional network to demonstrate its effectiveness. We used this energy estimation

pipeline to analyze the energy impacts of COVID-19 and congestions. To understand the energy impact of the COVID-19, we analyzed the road transportation-related energy reduction resulting from COVID-19 stay-at-home orders and found a total reduction of 3,213,515 gge/day (29.7%) in vehicle energy consumption. The results of the congestion energy impact analysis indicated that Class 8 trucks had larger energy loss ratio than passenger vehicles in the same congestion level, and that minor arterials and major collectors had the largest energy loss percentages.

This energy estimation pipeline provides a useful lens for transportation agencies, metropolitan planning organizations, and municipalities to assess road transportation- related energy consumption and energy impacts resulting from policy changes. The proposed energy estimation pipeline can also be used to aid in designing and implementing policies for reducing transportation-related energy consumption both during the ongoing COVID-19 pandemic and during the projected post-pandemic reopening phase. Moreover, this pipeline has the capacity to provide guidance on the future adoption of electric vehicles along with automated vehicles as well as to estimate how energy consumption will consequently be affected by changing fleet compositions. The capability of real-time vehicle energy consumption estimation can also be embedded in routing apps/algorithms enable real-time energy-efficient routing and better battery energy management for electric vehicles.

Although this energy estimation pipeline very accurately estimates hourly link-level vehicle energy, energy estimation models with an even finer temporal resolution (e.g., 5, 10, and 15 min) will be further explored in the future. The challenge of developing a sub-hourly model is the lack of reliable sub-hourly ground truth data

to valid the estimated results. Additional data sources, such as real-world vehicle composition data, will be included to further improve the model accuracy.

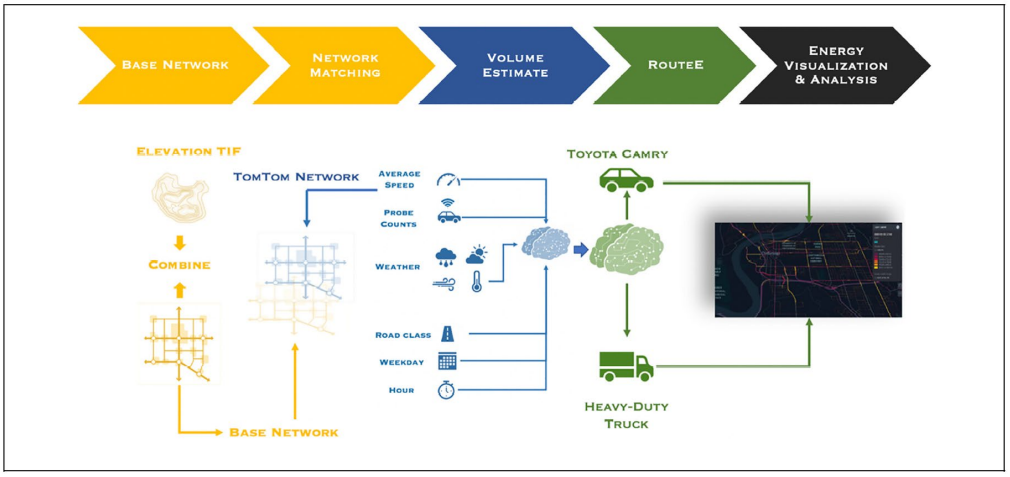


**Figure 1.** Link-level spatial-temporal resolved energy estimate pipeline.

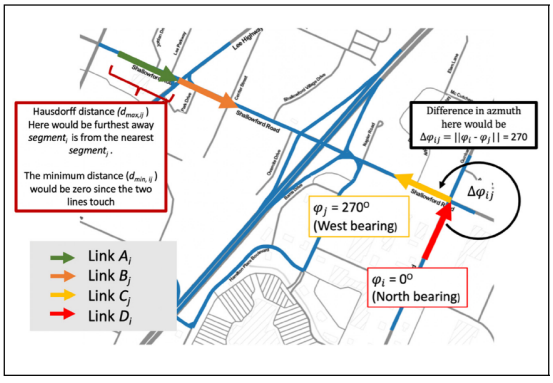


**Figure 2.** Visual example of the difference in azimuth of two road segments.

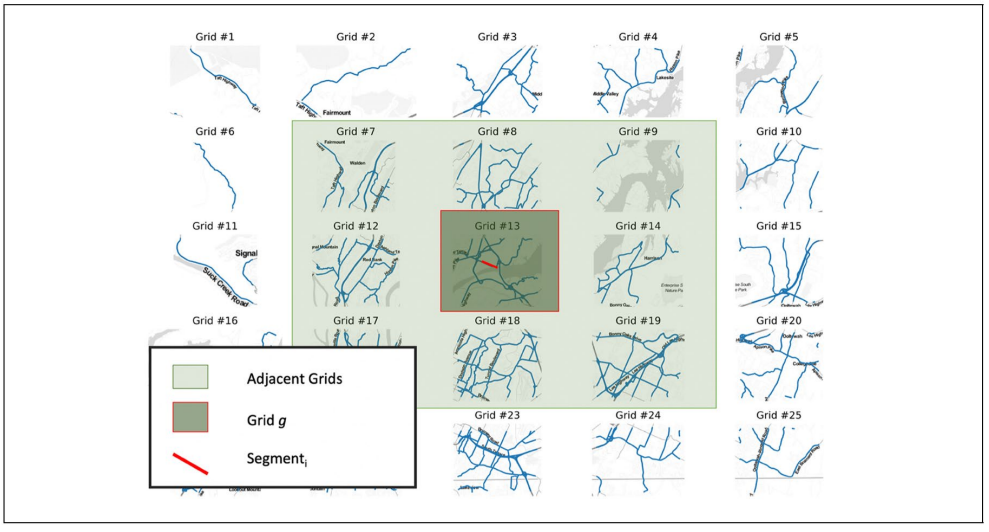


**Figure 3.** Example of partitioning networks into equal grids.

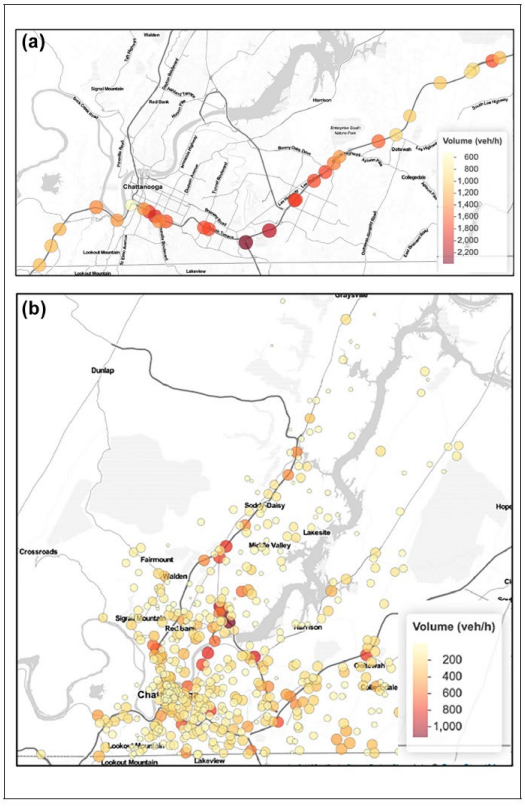


**Figure 4.** Traffic volume data collection locations: (*a*) interstate radar sensor locations and (*b*) non-interstate short-term count locations.

**Table 1.** Traffic Volume Estimation Data Sources

| Data type | Data source | Web link |
|---|---|---|
| Vehicle probe data | TomTom | https://developer.tomtom.com/traffic-stats |
| Weather | The Weather Company | https://www.ibm.com/weather |
| Short-term volume count | Tennessee DOT | https://www.tn.gov/tdot/long-range-planning-home/longrange-road-inventory/tn-times.html |
| Radar sensor data | Tennessee DOT | NA |

*Note*: DOT = Department of Transportation. NA = Not Available.

**Table 2.** Volume Estimation Model Performance Results

| Non-interstate model results | R-squared | Mean absolute error |
|---|---|---|
| Historical volume estimation | 0.77 | 76 |
| Real-time volume estimation | 0.76 | 79 |
| **Interstate model results** | **R-squared** | **Mean absolute error** |
| Historical volume estimation | 0.84 | 236 |
| Real-time volume estimation | 0.83 | 242 |

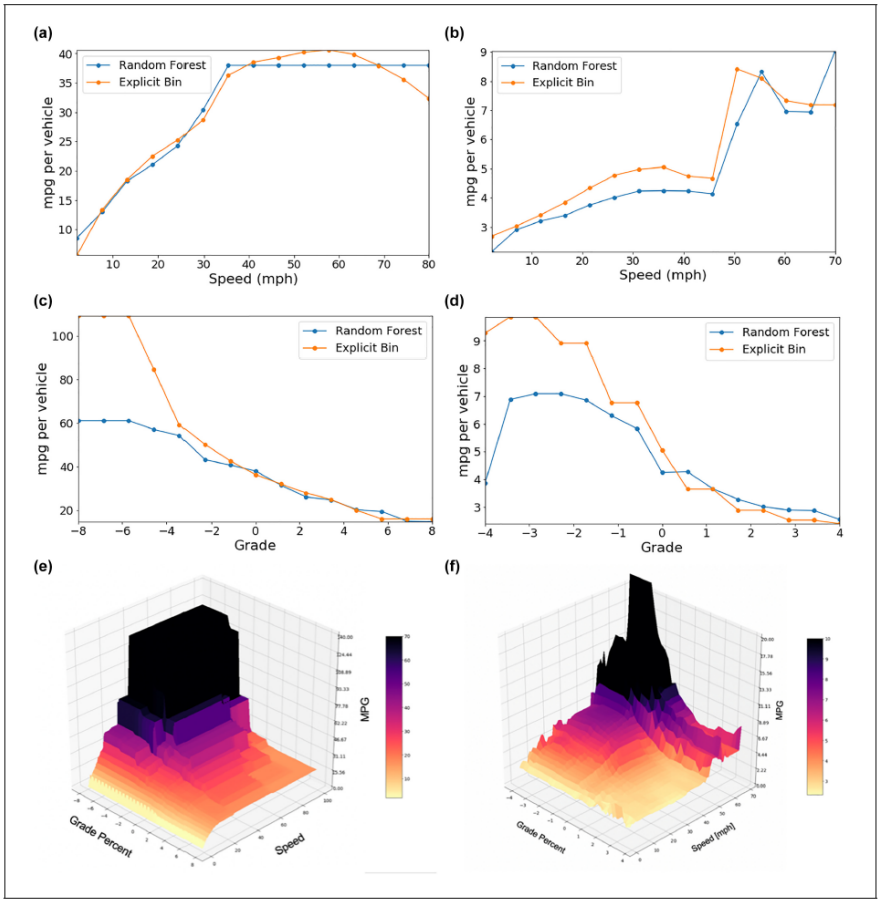


**Figure 5.** Analysis of RouteE models for Toyota Camry and Class 8 line-haul diesel truck models. Toyota Camry model: (a) Varied feature: speed (2 to 80 mph); fixed features: grade = 0%, link length = 0.2 mi (c) Varied feature: grade (28% to 8%) fixed features: Speed = 35 mph, link length = 0.2 mi (e) Varied features: speed (0 to 100 mph); grade (28% to 8%) fixed feature: link length = 1 mi Class 8 line-haul diesel truck model: (b) Varied feature: speed (2 to 70 mph) Fixed features: grade = 0%, link length = 0.2 mi (d) Varied feature: grade (24% to 4%) fixed features: speed = 35 mph, link length = 0.2 mi (f) Varied features: speed (0–70 mph); grade (24% to 4%) fixed feature: link length = 1 mi

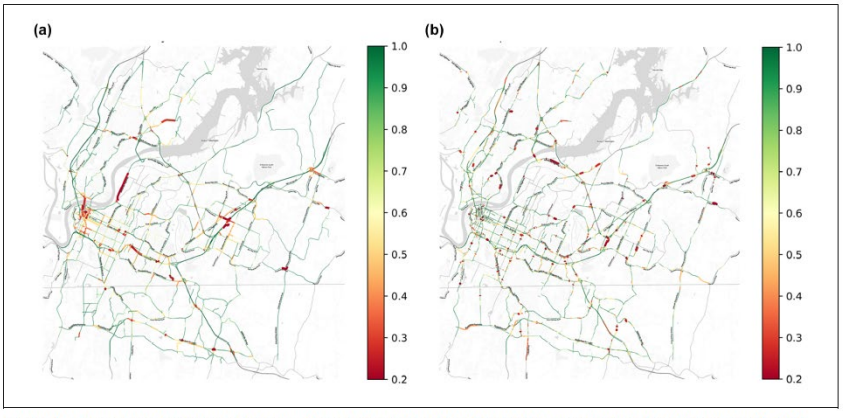


**Figure 6.** Comparison of real-time relative speeds near 6 p.m. before (*a*) and during (*b*) stay-at-home orders. (*a*) February 19, 2020 18:05:00 and (*b*) was March. 25, 2020 18:02:00.

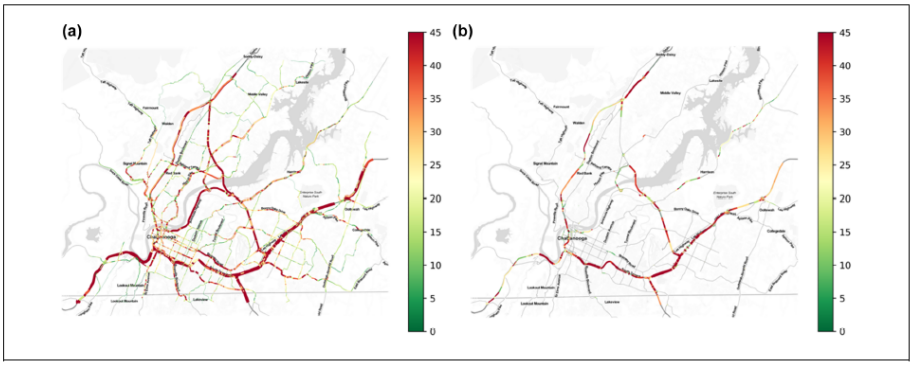


**Figure 7.** Energy intensity (gasoline gallon equivalent [gge] per mile) before (*a*) and during (*b*) COVID-19 stay-at-home orders.

**Table 3.** Total Reduction in Volume and Energy Consumption

| | Total VMT (vehicle miles traveled) of 24 h | | Total energy (gge) of 24 h | |
|---|---|---|---|---|
| | Highways | Arterials | Highways | Arterials |
| Before stay-at-home orders | 4523681 | 6301310 | 112874 | 169018 |
| During stay-at-home orders | 3227374 | 4384102 | 80030 | 116161 |
| % Change | −28.66 | −30.43 | −29.1 | −31.27 |
| Total % change | −29.69 | | −30.40 | |

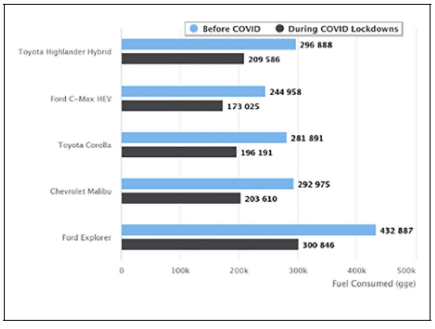


**Figure 8.** Comparing different vehicle models before and during COVID-19 stay-at-home orders.

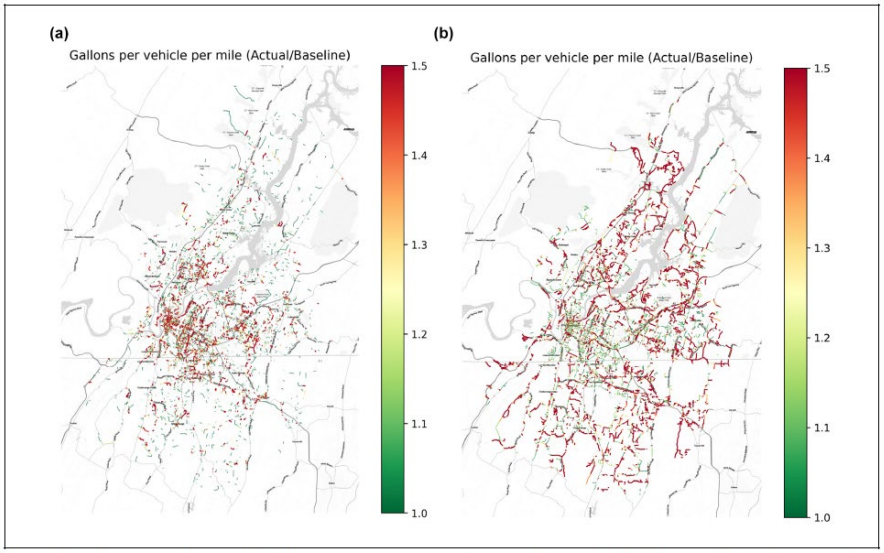


**Figure 9.** Link-wise energy loss ratio for Chattanooga road network at 5 p.m. on February 19th, 2020 using (*a*) Toyota Camry and (*b*) Class 8 line-haul truck models.

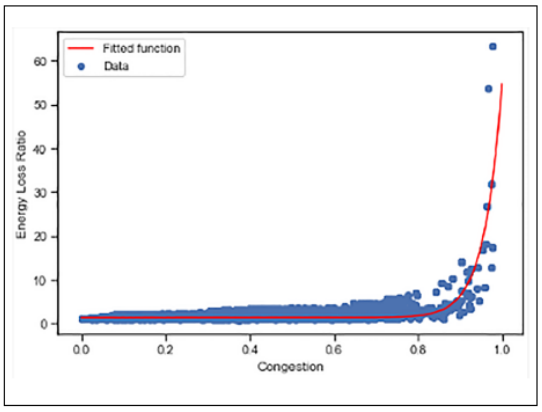


**Figure 10.** Exponential fit to energy loss ratio and congestion.


**Figure 11.** Link-level energy loss (gasoline gallon equivalent [gge] per mile) attributable to evening peak hour congestion.

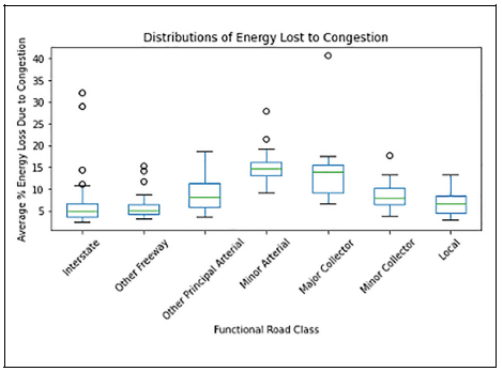


**Figure 12.** Average percentage of energy lost attributable to congestion by road class.

## References


1. U.S. Energy Information Administration. Monthly Energy Review. 2020.
2. U.S. Department of Energy Office of Energy Efficiency and Renewable Energy. Transportation Energy Futures – Combining Strategies for Deep Reductions in Energy Consumption and GHG Emissions, DOE/GO-102013-3845, 2013. https://www.nrel.gov/docs/fy13osti/56269.pdf
3. Ellis, D. and B. Glover. 2019 Urban Mobility Report.Texas A&M Transportation Institute, 2019. https://static.tti.tamu.edu/tti.tamu.edu/documents/mobility-report-2019-appx-c.pdf.
4. United Nations. 68% of the world population projected to live in urban areas by 2050, says UN. 2018. https://www.un.org/development/desa/en/news/population/2018-revisionof-world-urbanization-prospects.html.
5. Wang, J., I. Besselink, and H. Nijmeijer. Electric Vehicle Energy Consumption Modelling and Prediction Based on Road Information. World Electric Vehicle Journal, Vol. 7, No. 3, 2015, pp. 447–458.
6. Yuan, X., C. Zhang, G. Hong, X. Huang, and L. Li. Method for Evaluating the Real-World Driving Energy Consumptions of Electric Vehicles. Energy, Vol. 141, No. 15, 2017, pp. 1955–1968.
7. Miri, I., A. Fotouhi, and N. Ewin. Electric Vehicle Energy Consumption Modelling and Estimation—A Case Study. International Journal of Energy Research, Vol. 45, No. 1, 2021, pp. 501–520.
8. Lee, T. K., and Z. S. Filipi. Synthesis and Validation of Representative Real-World Driving Cycles for Plug-in Hybrid Vehicles. Proc., IEEE Vehicle Power and Propulsion Conference, Lille, 2010, pp. 1–6.
9. Wang, H., X. Zhang, and M. Ouyang. Energy Consumption of Electric Vehicles Based on Real-World Driving Pat- terns: A Case Study of Beijing. Applied Energy, Vol. 157, 2015, pp. 710–719.
10. TomTom. Traffic Stats Area Analysis. 2020. https://developer.tomtom.com/39traffic-stats/traffic-stats-apis/area-analysis.
11. Irani Ivanova. Google Maps to Provide ‘‘Eco-Friendly’’ Navigation Options. https://www.cbsnews.com/news/goo- gle-maps-eco-friendly-navigation/. Accessed April 7,2021
12. Ahn, K., and H. Rakha. The Effects of Route Choice Decisions on Vehicle Energy Consumption and Emissions. Transportation Research Part D: Transport and Environment, Vol. 13, No. 3, 2008, pp. 151–167.
13. Zhao, J., W. Li, J. Wang, and X. Ban. Dynamic Traffic Signal Timing Optimization Strategy Incorporating Various Vehicle Fuel Consumption Characteristics. IEEE Transactions on Vehicular Technology, Vol. 65, No. 6, 2015, pp. 3874–3887.
14. Al Islam, S. B., H. A. Aziz, and A. Hajbabaie. Stochastic Gradient-Based Optimal Signal Control with Energy Consumption Bounds. IEEE Transactions on Intelligent Transportation Systems, Vol. 22, No. 5, 2020, pp. 3054–3067.
15. De Cauwer, C., J. van Mierlo, and T. Coosemans. Energy Consumption Prediction for Electric Vehicles Based on Real-World Data. Energies, Vol. 8, 2015, pp. 8573–8593.
16. Wager, G., M. P. McHenry, J. Whale, and T. Bra¨unl. Testing Energy Efficiency and Driving Range of Electric Vehi- cles in Relation to Gear Selection. Renewable Energy, Vol. 62, 2014, pp. 303–312.
17. Dib, W., A. Chasse, P. Moulin, A. Sciarretta, and G. Corde. Optimal Energy Management for an Electric Vehicle in Eco-Driving Applications. Control Engineering Practice, Vol. 29, 2014, pp. 299–307.
18. Yao, E., Z. Yang, Y. Song, and T. Zuo. Comparison of Electric Vehicle’s Energy Consumption Factors for Differ- ent Road Types. Discrete Dynamics in Nature and Society, Vol. 2013, 2013, p. 328757.
19. Shankar, R., and J. Marco. Method for Estimating the Energy Consumption of Electric Vehicles and Plug-In Hybrid Electric Vehicles Under Real-World Driving Conditions. IET Intelligent Transport Systems, Vol. 7, 2013, pp. 138–150.
20. Yuksel, T., and J. J. Michalek. Effects of Regional Temperature on Electric Vehicle Efficiency, Range, and Emissions in the United States. Environmental Science & Technology, Vol. 49, No. 6, 2015, pp. 3974–3980.
21. Kambly, K. R., and T. H. Bradley. Estimating the HVAC Energy Consumption of Plug-In Electric Vehicles. Journal of Power Sources, Vol. 259, 2014, pp. 117–124.
22. Hassouna, F. M. A., and K. Al-Sahili. Future Energy and Environmental Implications of Electric Vehicles in Pales- tine. Sustainability, Vol. 12, No. 14, 2020, p. 5515.
23. Neaimeh, M., G. A. Hill, Y. Hu¨bner, and P. T. Blythe. Routing Systems to Extend the Driving Range of Electric Vehicles. IET Intelligent Transport Systems, Vol. 7, 2013, pp. 327–336.
24. Kraschl-Hirschmann, K., and M. Fellendorf. Estimating Energy Consumption for Routing Algorithms. Proc., IEEE 2012 Intelligent Vehicles Symposium, Alcala´de Henares, Spain, 2012.
25. Cappiello, A., I. Chabini, E. K. Nam, A. Lue, and M. A. Zed. A Statistical Model of Vehicle Emissions and Fuel Consumption. Proc., IEEE 5th International Conference on Intelligent Transportation Systems, Singapore, 2002.
26. Wu, X., X. He, G. Yu, A. Harmandayan, and Y. Wang. Energy-Optimal Speed Control for Electric Vehicles on Sig- nalized Arterials. IEEE Transactions on Intelligent Trans- portation Systems, Vol. 16, No. 5, 2015, pp. 2786–2796.
27. Yavasoglu, H. A., Y. E. Tetik, and K. Gokce. Implementation of Machine Learning Based Time Range Estimation Method Without Destination Knowledge for BEVs. Energy, Vol. 172, No. 1, 2019, pp. 1179–1186.
28. Ondruska, P., and I. Posner. Probabilistic Attainability Maps: Efficiently Predicting Driver-Specific Electric Vehi- cle Range. 2014 IEEE Intelligent Vehicles Symposium Proceedings, Dearborn, MI, 2014, pp. 1169–1174.
29. Karbowski, D., S. Pagerit, and A. Calkins. Energy Consumption Prediction of a Vehicle Along a User-Specified Real-World Trip. World Electric Vehicle Journal, Vol. 5, No. 4, 2012, pp. 1109–1120.
30. Zhang, R., and E. Yao. Electric Vehicles’ Energy Consumption Estimation with Real Driving Condition Data. Transportation Research Part D: Transport and Environment, Vol. 41, 2015, pp. 177–187.
31. Zhao, Q., Q. Chen, and L. Wang. Real-Time Prediction of Fuel Consumption Based on Digital Map API. Applied Sciences,

Vol. 9, No. 7, 2019, p. 1369.
32. Holden, J., N. Reinicke, and J. Cappellucci. RouteE: A Vehicle Energy Consumption Prediction Engine. No. 2020- 01-0939. SAE Technical Paper, 2020.
33. TSDC: Transportation Secure Data Center (2020). National Renewable Energy Laboratory. www.nrel.gov/ tsdc. Accessed January 15, 2020.
34. Zhang, Y., B. Yang, and X. Luan. Automated Matching Crowdsourcing Road Networks Using Probabilistic Relaxation. Proc., 2012 XXII ISPRS Congress, Melbourne, ViC, Australia, Vol. 25. 2012.
35. Zhang, M., L. Meng, and J. Bobrich. A Road-Network Matching Approach Guided by 'Structure'. Annals of GIS, Vol. 16, No. 3, 2010, pp. 165–176.
36. Fan, H., B. Yang, A. Zipf, and A. Rousell. A Polygon- Based Approach for Matching OpenStreetMapRoad Net- works with Regional Transit Authority Data. International Journal of Geographical Information Science, Vol. 30, No. 4, 2016, pp. 748–764.
37. Hou, Y., S. E. Young, A. Dimri, and N. Cohn. Network Scale Ubiquitous Volume Estimation Using Tree-Based Ensemble Learning Methods. Presented at 97th Annual Meeting of the Transportation Research Board, Washing- ton, D.C., 2018.
38. Hou, Y., and S. E. Young. Ubiquitous Traffic Volume Estimation for Lower Functional Class Roads. Presented at The Intelligent Transportation Society of America 2018 Annual Meeting, Detroit, MI, 2018.
39. Chen, T., and C. Guestrin. XGBoost: A Scalable Tree Boosting System. Proc., ACM SIGKDD International Conference on Knowledge Discovery and Data Mining, San Francisco, CA, 2016, pp.
785–794. https://doi.org/10.1145/2939672.2939785.
40. TomTom Developer Portal. Flow Segment Data. 2020. https://developer.tomtom.com/traffic-api/traffic-api-docu-mentation-traffic-flow/flow-segment-data.